



HAL
open science

Finite element reduced order model for noise and vibration reduction of double sandwich panels using shunted piezoelectric patches

Walid Larbi, Jean-François Deü, Roger Ohayon

► **To cite this version:**

Walid Larbi, Jean-François Deü, Roger Ohayon. Finite element reduced order model for noise and vibration reduction of double sandwich panels using shunted piezoelectric patches. *Applied Acoustics*, 2016, 108, pp.40-49. 10.1016/j.apacoust.2015.08.021 . hal-03177128

HAL Id: hal-03177128

<https://hal.science/hal-03177128v1>

Submitted on 16 Sep 2023

HAL is a multi-disciplinary open access archive for the deposit and dissemination of scientific research documents, whether they are published or not. The documents may come from teaching and research institutions in France or abroad, or from public or private research centers.

L'archive ouverte pluridisciplinaire **HAL**, est destinée au dépôt et à la diffusion de documents scientifiques de niveau recherche, publiés ou non, émanant des établissements d'enseignement et de recherche français ou étrangers, des laboratoires publics ou privés.

Finite element reduced order model for noise and vibration reduction of double sandwich panels using shunted piezoelectric patches

W. Larbi*, J.-F. Deü, R. Ohayon

*Structural Mechanics and Coupled Systems Laboratory,
Conservatoire National des Arts et Métiers,
292 rue Saint-Martin, 75141 Paris Cedex 03, France*

Abstract

This work concerns the control of sound transmission through double laminated panels with viscoelastic core using semi-passive piezoelectric shunt technique. More specifically, the system consists of two laminated walls, each one composed of three layers and called sandwich panel with an air cavity in between. The external sandwich panel has a surface-mounted piezoelectric patches. The piezoelectric elements, connected with resonant shunt circuits, are used for the vibration damping of some specific resonance frequencies of the coupled system. Firstly, a finite element formulation of the fully coupled visco-electro-mechanical-acoustic system is presented. This formulation takes into account the frequency dependence of the viscoelastic material. A modal reduction approach is then proposed to solve the problem at a lower cost. In the proposed technique, the coupled system is solved by projecting the mechanical displacement unknown on a truncated basis composed by the first real short-circuit structural normal modes and the pressure unknown on a truncated basis composed by the first acoustic modes with rigid boundaries conditions. The few initial electrical unknowns are kept in the reduced system. A static correction is also introduced in order to take into account the effect of higher modes. Various results are presented in order to validate and illustrate the efficiency of the proposed finite element reduced order formulation.

*Corresponding author. Email: walid.larbi@cnam.fr Tel. 0033140272793 Fax 0033140272502

Keywords: Double-wall, viscoelastic, vibroacoustic, finite element, modal reduction, piezoelectric shunt.

1. Introduction

Double-wall structures are widely used in noise control due to their superiority over single-leaf structures in providing better acoustic insulation. Typical examples include double glazed windows, fuselage of airplanes, panels of vehicles, etc. Various theoretical, experimental and numerical approaches have been investigated in the literature to predict the sound transmission through double walls with an acoustic enclosure. In [1, 2, 3], theoretical approaches are proposed for the derivation of the sound transmission factor of double panels of infinite size exposed to a random sound field as a function of frequency and angle of incidence. For a finite size flat panels, a theoretical study, based on Fourier series expansions, is presented in [4] concerning the vibroacoustic performance of a rectangular double-panel mounted in an infinite acoustic rigid baffle. Experimental evaluation of sound transmission through single, double and triple glazing can be found in [5, 6, 7, 8]. Regarding the numerical prediction approaches, several methods are available in the literature, such as the Finite Element Method (FEM), the Boundary Element Method (BEM), the Statistical Energy Analysis (SEA), etc. For all these approaches, the choice of the numerical method is related to the frequency band of interest (low, medium and high frequencies [9]). The SEA is generally used for high frequencies while in this work we are interested in the low and mid frequencies. In [10], the SEA is used for predicting sound transmission through double walls and for computing the non-resonant loss factor. In [11], FEM is applied to study the viscothermal fluid effects on vibro-acoustic behaviour of double elastic panels. The FEM is applied in [12] by the authors for the different layers of the sound barrier coupled to a variational BEM to account for fluid loading.

By introducing a thin viscoelastic interlayer within the panels, a better acoustic insulation is obtained. In fact, sandwich structures with viscoelastic layer are commonly used in many applications for vibration damping and noise control. In such structures, the main energy loss mechanism is due to the transverse shear of the viscoelastic core. However, accurate modeling of structures with viscoelastic materials is difficult because the measured dynamic properties of viscoelastic material are frequency and temperature

dependent. This motivated several authors to develop accurate numerical methods of modeling the effects of viscoelastic damping mechanisms which introduce frequency dependence. A review of these methods can be found in [13]. Concerning the application of these structures in noise attenuation, we can cite for example [8, 14].

In [8], the measured sound transmission loss of multilayered structures is compared with transfer matrix method results (assuming infinite layers) and a wave based model (taking into account finite dimensions) to show the importance of the finite dimensions in a broad frequency range. The effects of viscothermal fluid in a laminated double glazing are investigated in [14] using a finite element approach.

However, at low frequency, in particular around the mass-air-mass resonance of the double wall, the acoustic performance of this type of system is greatly deteriorated and the viscoelastic layer is not effective for treating the fall of the sound transmission loss. The aim of this work is to reduce the sound transmission at these resonance frequencies by a passive piezoelectric shunt technique through a full finite element modeling of the problem. In this technology, the elastic structure is equipped with piezoelectric patches that are connected to a passive electrical circuit, called a shunt. The piezoelectric patches transform mechanical energy of the vibrating structure into electrical energy, which is then dissipated by Joule heat in the shunt circuits. Several shunt circuits can be considered: the classical R- and RL-shunts, proposed by Hagood and Von Flotow [15] and improvements of those techniques, by the use of several piezoelectric elements [16, 17, 18], active fiber composites [19] or adaptive shunts [20], and recently semi-passive techniques, commonly known as switch techniques [21, 22, 23]. As those techniques are passive (or semi-passive if some electronic components have to be powered), a critical issue is that their performances, in terms of damping efficiency, directly depend on the electromechanical coupling between the host structure and the piezoelectric elements, which has to be maximized and necessitates the development of predictive models.

The present work concerns the numerical modeling of noise and vibration reduction of double laminated walls with viscoelastic interlayers by using shunted piezoelectric elements. The frequency domain of interest is the low and medium bands. The aim is to propose efficient reduced order finite element model able to predict the shunt damping around the mass-air-mass resonance of the system. In the first part of this paper, a finite element formulation of double-wall sandwich panels with viscoelastic core and

equipped with shunted piezoelectric patches is presented. This formulation involves structural displacement in the structure (sandwich structure with piezoelectric elements), acoustic pressure in the fluid cavity and the electric charge and voltage between the electrodes in the piezoelectric patches. The charge/voltage variables are intrinsically adapted to include any external electrical circuit into the electromechanical problem and to simulate the effect of shunt damping techniques. Moreover, since the elasticity modulus of the viscoelastic core is complex and frequency dependent, this formulation is complex and nonlinear in terms of frequency. The direct solution of this problem can be considered only to a model which does not imply a prohibitive number of degrees of freedom. This has severe limitations in attaining adequate accuracy and wider frequency ranges of interest. A reduced order-model is then proposed to solve the problem at a lower cost in the second part of this work. The proposed methodology, based on a normal mode expansion, requires the computation of the uncoupled structural and acoustic modes. The uncoupled structural modes are the real and undamped modes of the sandwich panels without fluid pressure loading at fluid-structure interface and with short-circuited patches, whereas the uncoupled acoustic modes are the cavity modes with rigid wall boundary conditions at the fluid-structure interface. Moreover, the effects of the higher modes of each subsystem are taken into account through an appropriate so-called a priori static correction based on adding the static modes, defined as the deformation shape at every load, to the truncated bases. It is shown that the projection of the full-order coupled finite element model on the uncoupled bases, leads to a reduced order model in which the main parameters are the classical fluid-structure coefficient, the residual stiffness complex coupling factors and the electromechanical coupling factors. Thanks to its reduced size, this model is proved to be very efficient for simulations of steady-state and frequency analyses of the fully coupled visco-electro-mechanical-acoustic system and the computational effort is significantly reduced. Note that the computing of eigenmodes in the medium frequency range presents no difficulty in this work. Indeed, the new numerical computing tools allow easy access to these modes which was not the case before. As a next step, the sound transmission through double walls is investigated. When the normal velocity distribution of the panel is known, the acoustic pressure field generated in the outward direction of the two plates can be calculated with the so-called Rayleigh integral for two-dimensional sound radiation. For this purpose, it is assumed that the double wall panel is placed in an infinite baffle. The normal incidence sound

transmission is chosen in order to evaluate the acoustic performances and the sound insulation of the double wall. In the last part, numerical examples are presented in order to validate and analyse results computed from the proposed formulations.

2. Finite element formulation of the fully coupled electromechanical-acoustic system

Consider a double-wall structure shown in Fig. 1. Each wall occupies a domain Ω_{Ei} , $i \in \{1, 2\}$ such that $\Omega_E = (\Omega_{E1}, \Omega_{E2})$, considered to be in equilibrium, is a partition of the whole structure domain. A prescribed force density \mathbf{f} is applied to the external boundary Γ_t of Ω_E . The acoustic enclosure is filled with a compressible and inviscid fluid occupying the domain Ω_F . The cavity walls are rigid except those in contact with the flexible wall structures noted Σ . It should be mentioned that fluid loading on the source and receiving side of the double panel is neglected in this work. In order to

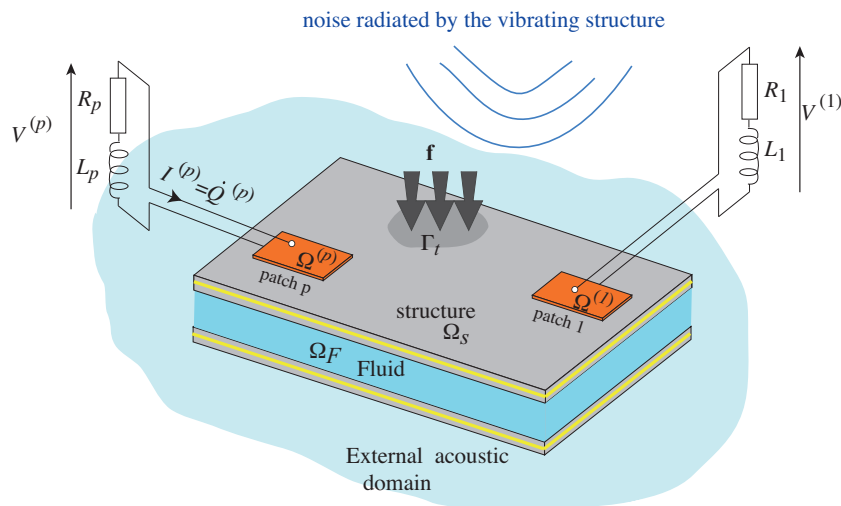


Figure 1: Double sandwich wall structure.

achieve maximum vibration dissipation and acoustic radiation attenuation of selected modes, the passive piezoelectric shunt damping technique is used. Thus, a set of P piezoelectric patches are bounded on the structure surface and connected to resistive or resonant shunt circuits. In this technology, the piezoelectric patches converts a fraction of mechanical energy associated

with the structure vibration into electrical energy, which is dissipated by heat through the resistor in the shunt circuits. Each piezoelectric patch has the shape of a plate with its upper and lower surfaces covered with very thin layer electrodes. The p th patch, $p \in \{1, \dots, P\}$, occupies a domain $\Omega^{(p)}$ such that $(\Omega_E, \Omega^{(1)}, \dots, \Omega^{(P)})$ is a partition of the all structure domain Ω_S . Moreover, we denotes by $R^{(p)}$ and $L^{(p)}$ the resistance and the inductance of the resonant shunt circuit connected to the p th patch.

For each piezoelectric patch, a set of hypotheses, which can be applied to a wide spectrum of practical applications, are formulated:

- The piezoelectric patches are thin, with a constant thickness, denoted $h^{(p)}$ for the p th patch;
- The thickness of the electrodes is much smaller than $h^{(p)}$ and is thus neglected;
- The piezoelectric patches are polarized in their transverse direction (i.e. the direction normal to the electrodes).

Under those assumptions, the electric field vector, of components $E_k^{(p)}$, can be considered normal to the electrodes and uniform in the piezoelectric patch [24], so that for all $p \in \{1, \dots, P\}$:

$$E_k^{(p)} = -\frac{V^{(p)}}{h^{(p)}} n_k \quad \text{in } \Omega^{(p)} \quad (1)$$

where E_i is the electric field, $V^{(p)}$ is the potential difference between the upper and the lower electrode surfaces of the p th patch which is constant over $\Omega^{(p)}$ and n_k is the k th component of the normal unit vector to the surface of the electrodes.

The harmonic local equations of this coupled problem can be written in terms of the structure displacement \mathbf{u} , the fluid pressure field p , the electric displacement \mathbf{D} and the electric field \mathbf{E} (the reader is referred to [25, 26] for more details about these equations). After variational formulation and finite element discretization, we obtain the following matrix system in frequency domain:

$$\begin{bmatrix} \mathbf{K}_u & \mathbf{C}_{uV} & -\mathbf{C}_{up} \\ -\mathbf{C}_{uV} & \mathbf{K}_V & \mathbf{0} \\ \mathbf{0} & \mathbf{0} & \mathbf{K}_p \end{bmatrix} \begin{bmatrix} \mathbf{U} \\ \mathbf{Q} \\ \mathbf{P} \end{bmatrix} - \omega^2 \begin{bmatrix} \mathbf{M}_u & \mathbf{0} & \mathbf{0} \\ \mathbf{0} & \mathbf{0} & \mathbf{0} \\ \mathbf{C}_{up}^T & \mathbf{0} & \mathbf{M}_p \end{bmatrix} \begin{bmatrix} \mathbf{U} \\ \mathbf{V} \\ \mathbf{P} \end{bmatrix} = \begin{bmatrix} \mathbf{F} \\ \mathbf{Q} \\ \mathbf{0} \end{bmatrix} \quad (2)$$

where \mathbf{U} is the column vector of nodal values of mechanical displacement of length M_s (M_s is the number of mechanical degrees of freedom); \mathbf{M}_u and \mathbf{K}_u are the mass and stiffness matrices of the structure (elastic structure and piezoelectric patches) of size $M_s \times M_s$; \mathbf{F} is the applied mechanical force vector of length M_s , \mathbf{P} is the column vector of nodal values of acoustic pressure of length M_f (M_f is the number of acoustic degrees of freedom); \mathbf{M}_p and \mathbf{K}_p are the mass and stiffness matrices of the fluid of size $M_f \times M_f$; \mathbf{C}_{up} is the fluid-structure coupled matrix of size $M_s \times M_f$. Moreover, $\mathbf{Q} = (Q^{(1)} Q^{(2)} \dots Q^{(P)})^T$ and $\mathbf{V} = (V^{(1)} V^{(2)} \dots V^{(P)})^T$ are the column vectors of electric charges and potential differences; \mathbf{C}_{uV} is the electric mechanical coupled stiffness matrix of size $M_s \times P$; $\mathbf{K}_V = \text{diag}(C^{(1)} C^{(2)} \dots C^{(P)})$ is a diagonal matrix filled with the P capacitances of the piezoelectric patches where $C^{(p)} = \epsilon_{33} S^{(p)} / h^{(p)}$, ϵ_{33} being the piezoelectric permittivity in the direction normal to the electrodes and $S^{(p)}$ the area of the patch electrodes surfaces.

The above discretized formulation equation is adapted to any elastic structure with surface-mounted piezoelectric patches. Its originality lies in the fact that the system electrical state is fully described by very few global discrete unknowns: only a couple of variables per piezoelectric patch, namely (1) the electric charge contained in the electrodes and (2) the voltage between the electrodes. Once the electrical part of the problem is fully discretized at the weak formulation step, by introducing the above cited voltage/charge variables, without any restriction on the mechanical part of the problem, any standard FE formulation can be easily modified to include the piezoelectric patches and thus the effect of an external electrical action. A second advantage of this formulation is that since global electrical variables are used, realistic electrical boundary conditions are naturally introduced. First, the equipotentiality in any of the patches electrodes is exactly satisfied when introducing the potential difference variable. Second, the use of the global charge contained in the electrodes, as the second electrical variable, is realistic since plugging an external electrical circuit to the electrodes of the patches imposes only the global charge contained in the electrodes and not a local charge surface density. Another advantage of using the global charge voltage variables is that they are intrinsically adapted to include any external electrical circuit into the electromechanical problem and to simulate the effect of shunt damping techniques. In this case, neither \mathbf{V} nor \mathbf{Q} is prescribed by the electrical network but the latter imposes only a relation between them [15]. For the case of a resonant shunt composed of a resistor R and an inductor L

in series, connected to the p th patch, the relation writes

$$-\omega^2 L^{(p)} Q^{(p)} + i\omega R^{(p)} Q^{(p)} + V^{(p)} = 0 \quad (3)$$

Combining equations (2) and (3), we finally obtain the general FE formulation of the electromechanical problem when the piezoelectric patches are shunted

$$-\omega^2 \begin{bmatrix} \mathbf{M}_u & \mathbf{0} & \mathbf{0} \\ \mathbf{0} & \mathbf{L} & \mathbf{0} \\ \mathbf{C}_{up}^T & \mathbf{0} & \mathbf{M}_p \end{bmatrix} \begin{bmatrix} \mathbf{U} \\ \mathbf{Q} \\ \mathbf{P} \end{bmatrix} + i\omega \begin{bmatrix} \mathbf{0} & \mathbf{0} & \mathbf{0} \\ \mathbf{0} & \mathbf{R} & \mathbf{0} \\ \mathbf{0} & \mathbf{0} & \mathbf{0} \end{bmatrix} \begin{bmatrix} \mathbf{U} \\ \mathbf{Q} \\ \mathbf{P} \end{bmatrix} + \begin{bmatrix} \mathbf{K}_u + \mathbf{C}_{uV} \mathbf{K}_V^{-1} \mathbf{C}_{uV}^T & \mathbf{C}_{uV} \mathbf{K}_V^{-1} & -\mathbf{C}_{up} \\ \mathbf{K}_V^{-1} \mathbf{C}_{uV}^T & \mathbf{K}_V^{-1} & \mathbf{0} \\ \mathbf{0} & \mathbf{0} & \mathbf{K}_p \end{bmatrix} \begin{bmatrix} \mathbf{U} \\ \mathbf{Q} \\ \mathbf{P} \end{bmatrix} = \begin{bmatrix} \mathbf{F} \\ \mathbf{0} \\ \mathbf{0} \end{bmatrix} \quad (4)$$

where $\mathbf{R} = \text{diag}(R^{(1)} R^{(2)} \dots R^{(P)})$ and $\mathbf{L} = \text{diag}(L^{(1)} L^{(2)} \dots L^{(P)})$ are the diagonal matrices filled with the electrical resistances and the electrical inductances of the shunt circuits. Note that since \mathbf{K}_V is diagonal, the evaluation of \mathbf{K}_V^{-1} is straightforward.

3. Viscoelastic core

In order to provide better acoustic insulation, damped sandwich panels with a thin layer of viscoelastic core are used in this study (Fig. 1). In fact, when subjected to mechanical vibrations, the viscoelastic layer absorbs part of the vibratory energy in the form of heat. Another part of this energy is dissipated in the constrained core due to the shear motion.

The constitutive relation for a viscoelastic material subjected to a sinusoidal strain is written in the following form:

$$\boldsymbol{\sigma} = \mathbf{C}^*(\omega) \boldsymbol{\varepsilon} \quad (5)$$

where $\boldsymbol{\varepsilon}$ denote the strain tensor and $\mathbf{C}^*(\omega)$ termed the complex moduli tensor, is generally complex and frequency dependent (* denotes complex quantities). It can be written as [9]:

$$\mathbf{C}^*(\omega) = \mathbf{C}'(\omega) + i\mathbf{C}''(\omega) \quad (6)$$

where $i = \sqrt{-1}$.

Furthermore, for simplicity, a linear, homogeneous and viscoelastic core will be used in this work. In the isotropic case, the viscoelastic material is defined by a complex and frequency dependent shear modulus in the form:

$$G^*(\omega) = G'(\omega) + iG''(\omega) \quad (7)$$

where $G'(\omega)$ is known as shear storage modulus, as it is related to storing energy in the volume and $G''(\omega)$ is the shear loss modulus, which represents the energy dissipation effects. The loss factor of the viscoelastic material is defined as

$$\eta(\omega) = \frac{G''(\omega)}{G'(\omega)} \quad (8)$$

which alternatively allows writing Eq. (7) as

$$G^*(\omega) = G'(\omega)(1 + i\eta(\omega)) \quad (9)$$

The Poisson's ratio ν is considered real and frequency independent. The loss factor of Young's modulus E^* is the same as that of the shear modulus, which leads to:

$$E^*(\omega) = E'(\omega)(1 + i\eta(\omega)) \quad (10)$$

where $E'(\omega) = 2G'(\omega)(1 + \nu)$.

With these assumptions, the stress tensor is complex and frequency dependent which makes the stiffness matrix of the sandwich structure complex and also frequency dependent. It will be noted $\mathbf{K}_u^*(\omega)$.

4. Reduced order model

The finite element model of Eq. (4) is applicable only to a model which does not imply a prohibitive number of degrees of freedom. To overcome these limitations, we present in this section, a reduced-order formulation for computing the frequency response functions of the fully coupled visco-electro-mechanical-acoustic system. The proposed approach is based on a normal mode expansion and truncation of high-frequency modes. The chosen reduction concerns only the mechanical and acoustical variables \mathbf{U} and \mathbf{P} . The electrical unknown field \mathbf{Q} is not concerned by the reduction because the dimension of this vector corresponds to the number of piezo-patches and therefore is very small compared to the mechanical (i.e., displacement in the host structure and the piezo-patches) and acoustical finite element degrees-of-freedom. The mechanical displacement unknown is projected on a truncated

basis composed by the first structural *in vacuo* modes with short-circuited patches while the acoustic pressure unknown is projected on a truncated basis composed by the first acoustic normal mode computed from the Helmholtz equation with rigid boundary conditions.

4.1. Eigenmodes of the structure in vacuo

In a first phase, the first N_s eigenmodes of the structure *in vacuo* with short-circuited patches are obtained from

$$[\mathbf{K}_u^*(\omega) - \omega^2 \mathbf{M}_u] \mathbf{U} = \mathbf{0} \quad (11)$$

Due to the frequency dependence of the stiffness matrix, this eigenvalue problem is complex and nonlinear. It is assumed that vibrations of the damped structure can be represented in terms of the real modes of the associated undamped system if appropriate damping terms are inserted into the uncoupled modal equations of motion [27, 28]. Thus, the complex stiffness matrix is decomposed in the sum of two matrices:

$$\mathbf{K}_u^*(\omega) = \mathbf{K}_{u0} + \delta \mathbf{K}_u^*(\omega) \quad (12)$$

where \mathbf{K}_{u0} is the real and frequency-independent stiffness matrix calculated with a constant Young's modulus of the viscoelastic core and $\delta \mathbf{K}_u^*(\omega)$ is the residual stiffness matrix.

The i th real eigenmode is obtained from the following equation

$$[\mathbf{K}_{u0} - \omega_{si}^2 \mathbf{M}_u] \Phi_{si} = \mathbf{0} \quad \text{for } i \in \{1, \dots, N_s\} \quad (13)$$

where (ω_{si}, Φ_{si}) are the natural frequency and eigenvector for the i th structural mode. These modes verify the following orthogonality properties

$$\Phi_{si}^T \mathbf{M}_u \Phi_{sj} = \delta_{ij} \quad \text{and} \quad \Phi_{si}^T \mathbf{K}_{u0} \Phi_{sj} = \omega_{si}^2 \delta_{ij} \quad (14)$$

where δ_{ij} is the Kronecker symbol and Φ_{si} have been normalized with respect to the structure mass matrix.

4.2. Eigenmodes of the internal acoustic cavity with rigid walls

In this second phase, the first N_f eigenmodes of the acoustic cavity with rigid boundary conditions are obtained from the following equation

$$[\mathbf{K}_p - \omega_{fi}^2 \mathbf{M}_p] \Phi_{fi} = \mathbf{0} \quad \text{for } i \in \{1, \dots, N_f\} \quad (15)$$

where (ω_{fi}, Φ_{fi}) are the natural frequency and eigenvector for the i th acoustic mode. These modes verify the following orthogonality properties

$$\Phi_{fi}^T \mathbf{M}_p \Phi_{fj} = \delta_{ij} \quad \text{and} \quad \Phi_{fi}^T \mathbf{K}_p \Phi_{fj} = \omega_{fi}^2 \delta_{ij} \quad (16)$$

where Φ_{fi} have been normalized with respect to the fluid mass matrix.

4.3. Modal expansion of the general problem

By introducing the matrices $\Phi_s = [\Phi_{s1} \cdots \Phi_{sN_s}]$ of size $(M_s \times N_s)$ and $\Phi_f = [\Phi_{f1} \cdots \Phi_{fN_f}]$ of size $(M_f \times N_f)$ corresponding to the uncoupled bases (M_s and M_f are the total number of degrees of freedom in the finite elements model associated to the structure and the acoustic domains respectively), the displacement and pressure are sought as

$$\mathbf{U} = \Phi_s \mathbf{q}_s(t) \quad \text{and} \quad \mathbf{P} = \Phi_f \mathbf{q}_f(t) \quad (17)$$

where the vectors $\mathbf{q}_s = [q_{s1} \cdots q_{sN_s}]^T$ and $\mathbf{q}_f = [q_{f1} \cdots q_{fN_f}]^T$ are the modal amplitudes of the structure displacement and the fluid pressure respectively.

Substituting these relations into Eq. (4) and pre-multiplying the first row by Φ_s^T and the third one by Φ_f^T , we obtain the equation

$$\begin{aligned} & \begin{bmatrix} \Phi_s^T (\mathbf{K}_{u0} + \delta \mathbf{K}_u^*(\omega) + \mathbf{C}_{uV} \mathbf{K}_V^{-1} \mathbf{C}_{uV}^T) \Phi_s & \Phi_s^T \mathbf{C}_{uV} \mathbf{K}_V^{-1} & -\Phi_s^T \mathbf{C}_{up} \Phi_f \\ & \mathbf{K}_V^{-1} \mathbf{C}_{uV}^T \Phi_s & \mathbf{0} \\ & \mathbf{0} & \Phi_f^T \mathbf{K}_p \Phi_f \end{bmatrix} \begin{bmatrix} \mathbf{q}_s \\ \mathbf{Q} \\ \mathbf{q}_f \end{bmatrix} \\ & + i\omega \begin{bmatrix} \mathbf{0} & \mathbf{0} & \mathbf{0} \\ \mathbf{0} & \mathbf{R} & \mathbf{0} \\ \mathbf{0} & \mathbf{0} & \mathbf{0} \end{bmatrix} \begin{bmatrix} \mathbf{U} \\ \mathbf{Q} \\ \mathbf{q}_f \end{bmatrix} - \omega^2 \begin{bmatrix} \Phi_s^T \mathbf{M}_u \Phi_s & \mathbf{0} & \mathbf{0} \\ \mathbf{0} & \mathbf{L} & \mathbf{0} \\ \Phi_f^T \mathbf{C}_{up}^T \Phi_s & \mathbf{0} & \Phi_f^T \mathbf{M}_p \Phi_f \end{bmatrix} \begin{bmatrix} \mathbf{q}_s \\ \mathbf{Q} \\ \mathbf{q}_f \end{bmatrix} \\ & = \begin{bmatrix} \Phi_s^T \mathbf{F} \\ \mathbf{0} \\ \mathbf{0} \end{bmatrix} \quad (18) \end{aligned}$$

This matrix equation represents the reduced order model of the fully coupled visco-electro-mechanical-acoustic system. If only few modes are kept for the projection, the size of this reduced order model ($N_s \times P \times N_f$) is much more smaller than the initial one ($M_s \times P \times M_f$). Eq. (18) can be also written in the following form of coupled differential equations:

- N_s mechanical equations

$$-\omega^2 q_{si} + \sum_{k=1}^{N_s} \alpha_{ik}^*(\omega) q_{sk} + \omega_{si}^2 q_{si} + \sum_{p=1}^P \sum_{k=1}^{N_s} \frac{\gamma_i^{(p)} \gamma_k^{(p)}}{C^{(p)}} q_{sk} + \sum_{p=1}^P \frac{\gamma_i^{(p)}}{C^{(p)}} Q^{(p)} - \sum_{j=1}^{N_f} \beta_{ij} q_{fj} = F_i \quad (19)$$

- P electric equations

$$-\omega^2 L^{(p)} Q^{(p)} + i\omega R^{(p)} Q^{(p)} + \frac{Q^{(p)}}{C^{(p)}} + \sum_{i=1}^{N_s} \frac{\gamma_i}{C^{(p)}} q_{si} = 0 \quad (20)$$

- N_f acoustic equations

$$-\omega^2 q_{fi} + \omega_{fi}^2 q_{fi} + \sum_{j=1}^{N_s} \beta_{ij} q_{sj} = 0 \quad (21)$$

where $F_i(t) = \Phi_{si}^T \mathbf{F}$ is the mechanical excitation of the i th mode; $\beta_{ij} = \Phi_{si}^T \mathbf{C}_{up} \Phi_{fj}$ is the fluid structure coupling coefficient, $\alpha_{ik}^*(\omega) = \Phi_{si}^T \Delta \mathbf{K}_u^*(\omega) \Phi_{sk}$ the reduced residual stiffness complex coefficient and $\gamma_i = \Phi_{si}^T \mathbf{C}_{uV}$ the electromechanical coupling factors.

At each frequency step, the reduced system (Eqs. (19), (20) and (21)) is solved by updating $\gamma_{ik}^*(\omega)$. After determining the complex amplitude vectors q_{si} and q_{fi} , the displacement and pressure fields are reconstructed using the modal expansion (Eqs. (17)).

4.4. Modal truncation augmentation method with static corrections

The process of mode truncation introduces some errors in the response that can be controlled or minimized by a modal truncation augmentation method. In this method, the effects of the truncated modes are considered by their static effect only.

First the applied loading vector \mathbf{F} is composed as:

$$\mathbf{F} = \sum_{i=1}^L \alpha_i(t) \mathbf{F}_{0i} \quad (22)$$

where \mathbf{F}_{0i} is the invariant spatial portion and $\alpha_j(t)$ is the time varying portion. For each invariant spatial load, the static modal eigenvector Ψ_{si} is given by:

$$\Psi_{si} = \mathbf{K}_{u0}^{-1} \mathbf{F}_{0i} \quad (23)$$

The truncated basis containing the real and undamped structure modes is enriched by the static modal eigenvectors such that

$$\bar{\Phi}_s = [\Phi_{s1} \cdots \Phi_{sN_s}, \Psi_{si}, \cdots \Psi_{sl}] = [\Phi_s \Psi_s] \quad (24)$$

The truncated fluid basis is enriched with the static pressure \mathbf{P}_s computed from the following equation (see [29, 30] for more details)

$$p^s = -\frac{\rho_F c_F^2}{|\Omega_F|} \int_{\Sigma} \mathbf{u} \cdot \mathbf{n} \, ds \quad (25)$$

Thus, the enriched fluid basis is

$$\bar{\Phi}_f = [\Phi_f \mathbf{P}_s] \quad (26)$$

The displacement and pressure are sought as

$$\mathbf{U} = \Phi_s \mathbf{q}_s(t) + \Psi_s \mathbf{q}_s^0(t) \quad \text{and} \quad \mathbf{P} = \Phi_f \mathbf{q}_f(t) + \mathbf{P}_s q_f^0(t) \quad (27)$$

where the vectors \mathbf{q}_s^0 and q_f^0 are the quasi-static modal amplitudes of the structure displacement and the fluid pressure respectively.

Substituting these relations (Eq. (27)) into Eq. (4) and pre-multiplying the first row by $\bar{\Phi}_s^T$ and the second one by $\bar{\Phi}_f^T$, we obtain coupled differential equations enriched with fluid and structure static modes similar than Eqs. (19) to (21) which are not shown here for the sake of brevity.

5. Acoustic indicators

In order to evaluate the acoustic performances and the sound insulation property of the double-wall sandwich panels, the radiated sound power (Π_t) and the normal incidence sound transmission loss (nSTL) are used as acoustic indicators in this work.

5.1. Radiated sound power

The radiated (or transmitted) sound power through the area S_2 of the panel Ω_{S_2} is given by:

$$\Pi_t = \frac{1}{2} \text{Re} \left(\int_{S_2} p(G) v_n^*(G) dS \right) \quad (28)$$

where G is a point on the plate surface Ω_{S_2} , p is the sound pressure applied as an external loading, v_n is the normal velocity (\star denotes the complex conjugate) and Re is the real part of the expression.

For a flat plate embedded in an infinite rigid plane baffle and radiating in a semi infinite fluid, p can be obtained using the Rayleigh Integral [3]:

$$p(\omega, M) = \rho_0 \frac{i\omega}{2\pi} \int_{S_2} v_n(\omega, G) \frac{e^{-ikr}}{r} dS \quad (29)$$

where ρ_0 is the mass density of the external acoustic domain, k is the wave number expressed as ω/c_0 , c_0 is the acoustic speed of sound, M is a point inside the external acoustic domain and $v_n(\omega, G)$ is the normal velocity at point G . Note that the normal velocity distribution on the structure can be easily obtained from the previous finite element formulation.

The baffled panel is divided into a grid of R rectangular elements with equal size whose transverse vibrations are specified in terms of the normal velocities at their centre positions. Assuming that the dimensions of the element are small compared with both the structural wavelength and the acoustic wavelength, the total radiated sound power (Eq. (28)) can then be expressed as the summation of the powers radiated by each element, so that

$$\Pi_t = \frac{S_e}{2} \text{Re} (\mathbf{v}_n^H \mathbf{p}) \quad (30)$$

where the superscript H denotes the hermitian transpose, \mathbf{v}_n and \mathbf{p} are the vectors of complex amplitudes of the normal volume velocity and acoustic pressure in all elements and S_e is the area of each element. The pressure on each element is generated by the vibrations of all elements of the panel. The vector of sound pressure can therefore be expressed by the impedance matrix relation

$$\mathbf{p} = \mathbf{Z} \mathbf{v}_n \quad (31)$$

where \mathbf{Z} is the matrix incorporating the point and transfer acoustic impedance terms over the grid of elements into which the panel has been subdivided:

$Z_{ij} = (i\omega\rho_0 S_e/2\pi r_{ij})e^{-ikr_{ij}}$ (r_{ij} is the distance between the centres of the i -th and j -th elements). Note that, because of reciprocity, the impedance matrix \mathbf{Z} is symmetric. Substituting Eq. (31) into the expression for the total radiated sound power given in Eq. (30), we obtain

$$\Pi_t = \frac{S_e}{2} \text{Re}(\mathbf{v}_n^H \mathbf{Z} \mathbf{v}_n) = \frac{S_e}{4} \text{Re}(\mathbf{v}_n^H [\mathbf{Z} + \mathbf{Z}^H] \mathbf{v}_n) = \mathbf{v}_n^H \mathbf{R} \mathbf{v}_n \quad (32)$$

The matrix \mathbf{R} is defined as the "radiation resistance matrix" for the elementary radiators which, for the baffled panel, is given by

$$\mathbf{R} = \frac{\omega^2 \rho_0 S_e^2}{4\pi c_0} \begin{bmatrix} 1 & \frac{\sin(kr_{12})}{kr_{12}} & \dots & \frac{\sin(kr_{1R})}{kr_{1R}} \\ \frac{\sin(kr_{21})}{kr_{21}} & 1 & \dots & \frac{\sin(kr_{2R})}{kr_{2R}} \\ \vdots & \vdots & \ddots & \vdots \\ \frac{\sin(kr_{R1})}{kr_{R1}} & \frac{\sin(kr_{R2})}{kr_{R2}} & \dots & 1 \end{bmatrix} \quad (33)$$

This method can be applied to any plane surface in an infinite baffle, independently of the boundary conditions. It only requires the knowledge of the surface geometry, the characteristics of the fluid and the velocity field distribution. In this work, a finite element approach is used to evaluate this velocity field by using a sufficient number of discrete radiating elements according to the smallest wavelength to be observed.

5.2. Normal incidence sound transmission loss

The normal incidence sound transmission of the double-wall sandwich panels is investigated in this section using Rayleigh Integral method described above. It is evaluated using the following formula:

$$nSTL = 10 \text{Log} \frac{\Pi_i}{\Pi_t} \quad (34)$$

where Π_i and Π_t are the incident and transmitted acoustic power respectively. For normal plane wave applied to plate Ω_{S1} , the incident sound power is given by:

$$\Pi_i = \frac{|P_{inc}|^2 S_1}{2\rho_0 c_0} \quad (35)$$

where P_{inc} represents the normal incident sound pressure amplitude and S_1 is the area of the whole panel Ω_{S1} .

6. Numerical examples

In this last section, numerical results, obtained with a Matlab program developed by the authors, are proposed in order to validate and analyse results computed from the proposed formulation. The first example concerns sound transmission through a double-plate system filled with air. In this example, we analyse the air gap effect on the natural vibration of the coupled system and the sound attenuation. The accuracy of model predictions is checked against existing test data. In the second example, the transmission loss factor of a double laminated glazing panel with a thin interlayer of PVB is presented. The mass-air-mass resonance is controlled with shunted piezoelectric patches. This last example shows also the performance of the proposed modal reduction method compared to direct approach and analyzes the effect of the damped piezo system and PVB (Polyvinyl Butyral) viscoelastic layer on noise attenuation.

6.1. Sound transmission through an elastic double-panel system

The problem under consideration is shown in Fig. 2. A normal incidence plane wave excites a double-plate system filled with air (density $\rho_F = 1.21$ kg/m³ and speed of sound $c_F = 340$ m/s). The plane wave has a pressure amplitude of 1 N/m² and is applied to plate 1 as the only external force to the system. The plates are identical and simply supported with thicknesses of 1 mm. The density of the plates is 2814 kg/m³, the Youngs modulus is 71 GPa, the Loss factor is 0.01 and Poisson ratio 0.33. The surrounding fluid is the air. This example was originally proposed by Panneton in [31].

Concerning the finite element discretization, we have used, for the structural part, 10×10 rectangular elements for each plate. The acoustic cavity is discretized using $10 \times 10 \times 5$ hexahedric elements. The structural and acoustic meshes are compatible at the interface. For more details about the used fluid and structure finite elements and the associated fluid-structure coupling element, we refer the reader to [32].

When the excitation is applied to the first plate, the second one vibrates and radiates sound caused by the coupling of air and plate 1. The normal incidence sound transmission loss is then computed using the Rayleigh's integral method which needs the finite element solution of surface velocities of plate 2. For this purpose, the resolution of the coupled system is done with a modal reduction approach using the first 10 in vacuo structural modes and the first 10 acoustic modes of the fluid in rigid cavity.

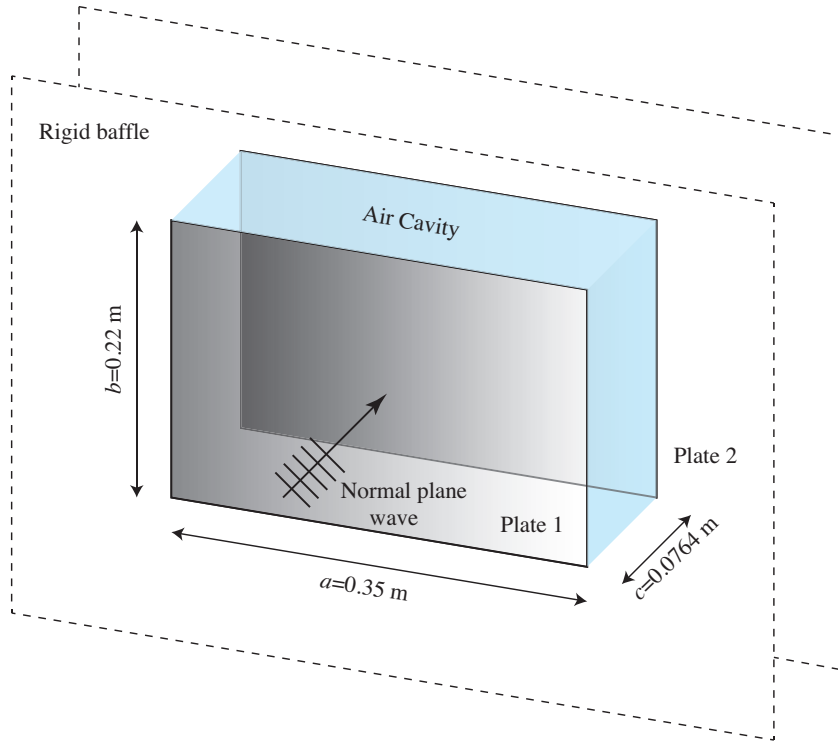


Figure 2: Double-plate system filled with air: geometric data.

Mode	Nastran	Matlab	Type of mode
(1, 1)	68.69	69.14	structure
(1, 1)*	153.58	148.79	coupled
(3, 1)	220.75	224.39	structure
(1, 3)	462.50	464.72	structure

Table 1: List of the coupled mode eigenfrequencies.

Fig. 3 shows the normal incidence transmission loss through a simply supported plate (dashed line). Due to the modal behavior of the plate, dips in the transmission loss curve are observed at its resonance frequencies (modes (1, 1), (3, 1) and (1, 3)). When a second plate is used to form an airtight cavity (continuous line), an increase in the transmission loss is achieved except in the region of the so-called plate-cavity-plate resonance (mode (1, 1)*). At this frequency, the two plates move out of phase with each

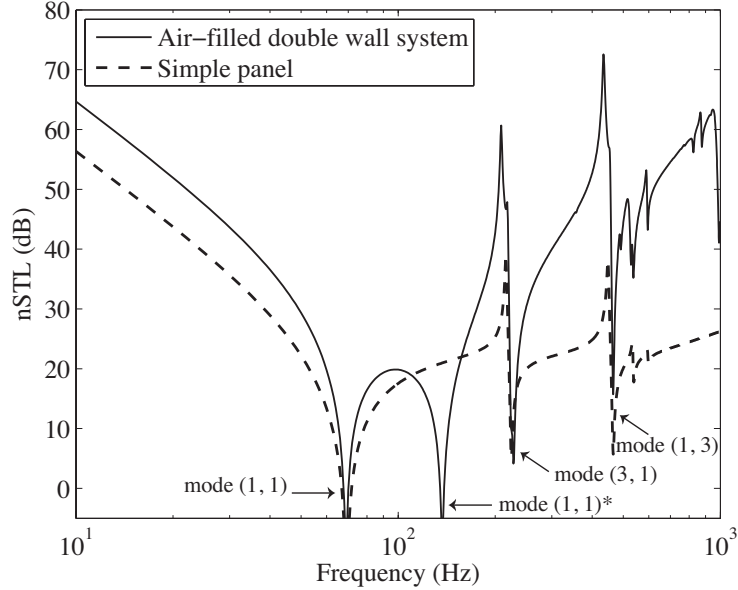


Figure 3: Comparison of the normal incidence sound transmission (nSTL) through an air-filled double panel and a simple panel.

other and the effect of the cavity on the plates is mostly one of added stiffness. This frequency is similar to the mass-air-mass resonance of unbounded double panels analyzed in the next section. The frequencies of these coupled modes are presented in Table 1. Table 1 shows also a comparison between results computed with the developed finite elements in Matlab and those given by the finite element code Nastran using the same mesh. These results show the excellent performance of the developed finite element model compared to Nastran and enable us to check the validity of the fluid-structure proposed formulation. In addition, the variation of the nSTL of an air-filled panels and a simple panel is in very good agreement with the published data from [31] which validates the development of the proposed acoustic indicators. Note that the influence of several key parameters on the sound isolation capability of the double-panel configuration including panel dimensions, thickness of air cavity, elevation angle, and azimuth angle of incidence sound is not the purpose of this study and can be found in [4].

Fig. 4 presents a comparison of the normal incidence sound transmission through an air-filled finite double panel and an air-filled infinite double panel

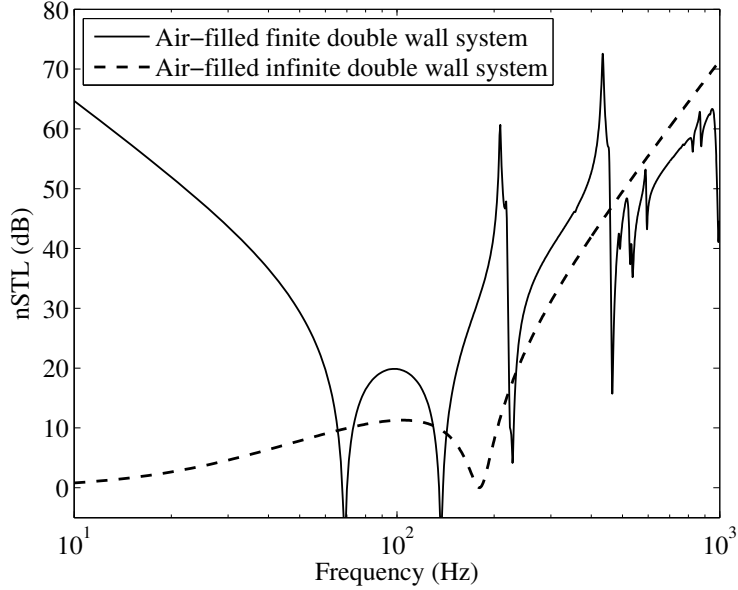


Figure 4: Comparison of the normal incidence sound transmission (nSTL) through an air-filled finite double panel (finite element result) and an air-filled infinite double panel (analytical solution).

computed from an analytical solution given in [3, 33]. For unbounded panels, the first dip occurs at the mass-air-mass frequency ($f_{mam} = 181.63$ Hz) given by the formula:

$$f_{mam} = \frac{1}{2\pi} \sqrt{\frac{\rho_F c_F^2}{d} \frac{m_{S1} + m_{S2}}{m_{S1} m_{S2}}} \quad (36)$$

where d is the panel spacing and m_{S1} and m_{S2} are the surface mass densities of the panels.

At this frequency, the two plates vibrate, as it were, on the stiffness of the air layer. For low frequencies up to the mass-air-mass frequency, the transmission loss follows the so-called mass law: the two plates are coupled in such a way that the plates vibrate as if they were a single plate with the total mass of the two plates and the transmission loss increasing with frequency at 6 dB per octave and 6 dB when the mass is doubled. It's clear from this comparison that the unbounded model is attractive to use for the prediction of global trends at higher frequencies, but is unsuitable to use for predictions in the small frequency bands and around eigenfrequencies of the

double wall panel [33].

6.2. Control of sound transmission through a double laminated glazing panels

The proposed reduced order finite-elements formulation is applied now to simulate the control of sound transmission through a double laminated glazing panels using shunted piezoelectric patches. The system consists of two identical clamped laminated panels of glass (in-plane dimensions are $L_x = 1.25$ m and $L_y = 1.5$ m) separated by an air cavity of 12 mm thickness. Each laminated glass is composed of two glass plates bonded together by a PVB interlayer. The thickness of outer and inner glass ply is $h_1 = h_3 = 3$ mm and those of the PVB interlayer is $h_2 = 1.14$ mm (figure 5).

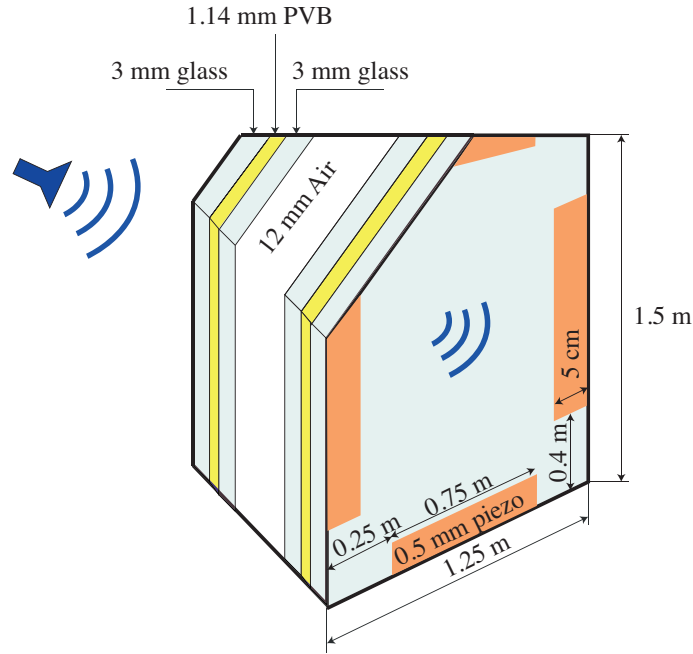


Figure 5: Double laminated glazing panels: geometric data.

The glass ply is modeled as linear elastic material (density 2500 kg/m^3 , Youngs modulus 72 GPa , and Poisson ratio 0.22). The material properties of the PVB are both thermal and frequency dependent. From dynamic and thermal tests, Havrillak and Negami have found an empirical law describing this dependence. The resulting complex frequency dependent shear modulus

of the PVB is given at 20°C as [34, 35]:

$$G^*(\omega) = G_\infty + (G_0 - G_\infty) [1 + (i\omega\tau_0)^{1-\alpha_0}]^{-\beta_0} \quad (37)$$

where $G_\infty = 0.235$ GPa, $G_0 = 0.479$ Mpa, $\alpha_0 = 0.46$, $\beta_0 = 0.1946$, $\tau_0 = 0.3979$. The Poisson ratio of the PVB is 0.4 and density is 999 kg/m³.

Concerning the laminated wall composed of three layers, the skins are supposed homogeneous, orthotropic and linearly elastic, with constant thickness and Kirchhoff-Love assumptions are made. The core is supposed linearly viscoelastic and subjected to the first order shear deformation theory. The stiffness and mass matrices are calculated using the finite element method (taking into account the rotational inertia effect in the mass matrix). Regarding the excitation and the mesh, we used the same ones as in the previous example.

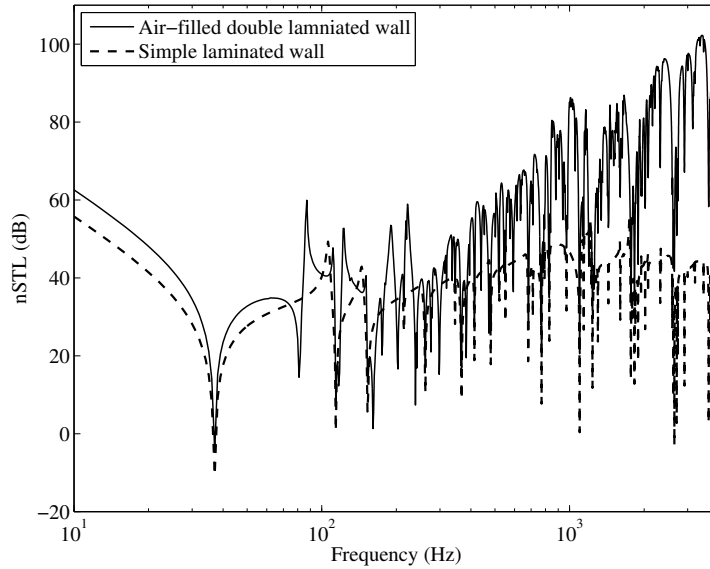


Figure 6: Comparison of the normal incidence sound transmission (nSTL) through an air-filled double laminated panel and a single laminated panel.

A comparison between a simple and a double laminated glass with PVB interlayer is shown in Fig. 6. Calculation was limited to 4000 Hz maximum. As mentioned in the first example, the second dip associated with the two

partitions is a phenomenon owned by the double-panel system and it is caused by the air cavity coupling effect that is absent in the single-panel system. Note that, from a comparison between conventional glass and laminated glass that is not shown here, the effect of the viscoelastic layer in noise reduction is more important in high frequencies than low frequencies. In fact, at low frequencies, the viscoelastic material is soft and the damping is small. At higher frequencies, the stiffness decreases rapidly and the damping is highest. Moreover, flexural vibrations cause shear strain in the viscoelastic core which dissipates energy and reduces vibration and noise radiation.

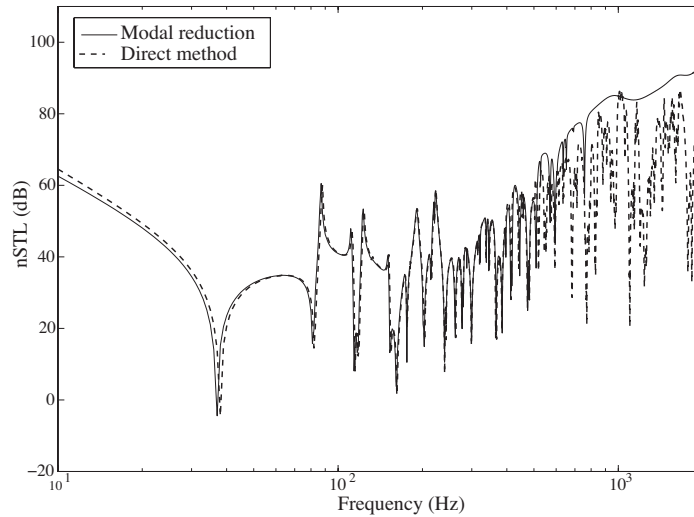


Figure 7: nSTL through an air-filled double panel: comparison between the modal reduction approach and the direct nodal method.

Fig. 7 shows a comparison between the nSTL of the coupled problem, obtained with the proposed modal reduction approach with a truncation on the first twenty structural modes ($N_s = 20$) and first twenty acoustic modes ($N_f = 20$) and the direct nodal method where the displacement and pressure vectors are calculated for each frequency step. The structural modes are calculated from Eq. (13) using the constant shear storage modulus G_∞ . As can be seen, a very good agreement between the two methods is proved. Note that, in order to evaluate the number of modes to keep in the modal projection, various simulations have been performed with the proposed static correction and twenty were sufficient by comparison with direct finite element

analysis in the frequency range of interest. In this respect, the resulting reduction of the model size and the computational effort using the reduced order method are very significant compared to those of the direct approach.

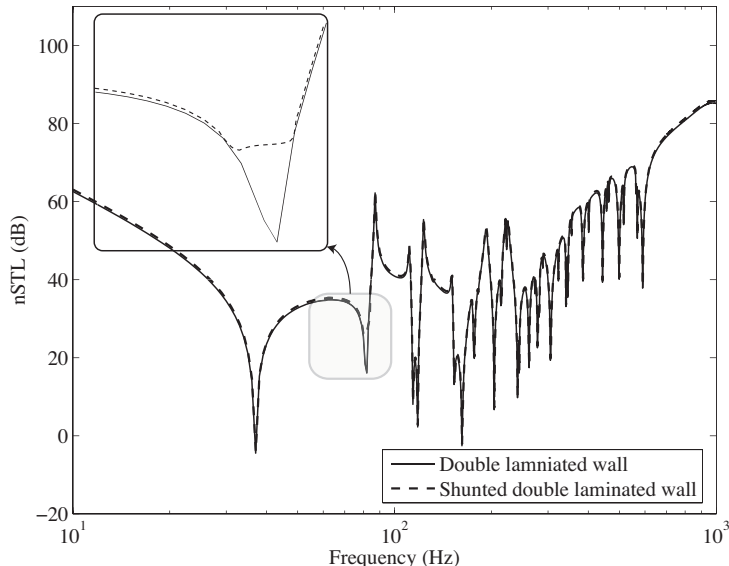


Figure 8: Normal sound transmission loss of laminated double panels: control of panel-air-panel resonance by shunted piezoelectric patches

In order to reduce the sound transmission around the mass-air-mass resonance of the double wall, four very thin identical piezoelectric patches (length 75 cm, width 5 cm, thick 0.5 mm) are mounted on the second wall (free on any mechanical charge) and tuned to an RL shunt circuit (see figure 5). The patch is composed from piezoelectric Macro Fiber Composite (MFC). The material properties of the MFC are: $E_1=30$ GPa, $E_2=15.5$ GPa, $E_3=15.5$ GPa, $G_{13}=10.7$ GPa, $G_{23}=10.7$ GPa, $G_{12}=5.7$ GPa, $\nu_{13}=0.4$, $\nu_{12}=0.35$, $d_{33} = 4.18 \times 10^{-10}$ m/V, $d_{32} = d_{31} = -1.98 \times 10^{-10}$ m/V, $\rho = 4700$ kg/m³.

The resistance R and the inductance L can be adjusted and properly chosen to maximize the damping effect of this particular mode. The optimal resistance and inductance of the i th mode for a series resonant shunt are

given by [15]:

$$R^{\text{opt}} = \frac{\sqrt{2k_{\text{eff},i}^2}}{C\omega_i(1 + k_{\text{eff},i}^2)} \quad (38\text{a})$$

$$L^{\text{opt}} = \frac{1}{C\omega_i^2(1 + k_{\text{eff},i}^2)} \quad (38\text{b})$$

where ω_i is the short circuit natural frequency of the i th mode, C is the capacitance of the piezoelectric patch and $k_{\text{eff},i}$ is the effective electromechanical modal coupling factor (EEMCF), characterizing the energy exchanges between the mechanical structure and the piezoelectric patches and defined by:

$$k_{\text{eff},i}^2 = \frac{\hat{\omega}_i^2 - \omega_i^2}{\omega_i^2} \quad (39)$$

and where $\hat{\omega}_i$ is the open-circuited natural frequency. For the chosen mode, the optimal values of the shunt electrical parameters are then, $R=743 \Omega$ and $L=67 \text{ H}$.

Fig. 8 presents the nSTL of the laminated double wall with and without piezoelectric shunt. The response is calculated with a modal reduction approach using the first 20 in vacuo structural modes and the first 20 acoustic modes of the fluid in rigid cavity with static correction. It can be seen that the resonant magnitude of the second mode (the mass-air-mass resonance) has been significantly reduced. In fact, the strain energy contained in the piezoelectric material is converted into electrical energy and hence dissipated into heat using the RL shunt device.

7. Conclusions

In this paper, a finite element formulation for semi-passive sound transmission reduction through double wall sandwich panels with viscoelastic core is presented. A reduced-order model, based on a normal mode expansion, is then developed. The proposed methodology requires the computation of the uncoupled eigenmodes of the undamped structure with short-circuit conditions, and the rigid acoustic cavity. Static corrections are introduced in the modal bases in order to take into account the effect of the higher modes. Despite its reduced size, this model is proved to be very efficient for simulations of steady-state analyses of structural-acoustic coupled systems with

viscoelastic interlayers and with shunt damping when appropriate damping terms are inserted into the modal equations of motion. The Rayleigh integral method is used in order to estimate the normal sound transmission loss factor of the system. Numerical examples are finally presented in order to evaluate the effectiveness of the proposed finite element reduced order model in terms of prediction of the vibration attenuation using piezoelectric shunt systems.

References

- [1] L.L. Beranek, G.A. Work, "Sound transmission through multiple structures containing flexible blankets", *Journal of the Acoustical Society of America*, 21(4), Pages 419-428, 1949.
- [2] A. London, "Transmission of reverberant sound through double walls", *Journal of the Acoustical Society of America*, 22(2), Pages 270-279, 1950.
- [3] F. Fahy, P. Gardonio "Sound and structural vibration: Radiation, Transmission and Response", Academic Press, 2006.
- [4] F. X. Xin, T.J. Lu, C.Q. Chen, "Vibroacoustic behavior of clamp mounted double-panel partition with enclosure air cavity", *Journal of the Acoustical Society of America*, 124(6), Pages 3604-3612, 2008.
- [5] J.D. Quirt, "Sound transmission through windows I. Single and double glazing", *Journal of the Acoustical Society of America*, 72(3), Pages 834-844, 1982.
- [6] J.D. Quirt, "Sound transmission through windows II. Double and triple glazing", *Journal of the Acoustical Society of America*, 74(2), Pages 534-542, 1983.
- [7] A.J.B. Tadeu, Diogo M.R. Mateus, "Sound transmission through single, double and triple glazing. Experimental evaluation", *Applied Acoustics*, 62, Pages 307-325, 2001.
- [8] A. Dijckmans, G. Vermeir, W. Lauriks, "Sound transmission through finite lightweight multilayered structures with thin air layers", *Journal of the Acoustical Society of America*, 128(6), Pages 3513-3524, 2010.

- [9] R. Ohayon, C. Soize, “Advanced computational vibroacoustics: Reduced-order models and uncertainty quantification”, Cambridge University Press, 2014.
- [10] R.J.M. Craik, “Non-resonant sound transmission through double walls using statistical energy analysis”, *Applied Acoustics* 64, Pages 325-341, 2003.
- [11] A. Akrouf, C. Karra, L. Hammami, M. Haddar, “Viscothermal fluid effects on vibro-acoustic behaviour of double elastic panels”, *International Journal of Mechanical Sciences*, 50(4), Pages 764-773, 2008.
- [12] F.C. Sgard, N. Atalla, J. Nicolas, “A numerical model for the low frequency diffuse field sound transmission loss of double-wall sound barriers with elastic porous linings”, *Journal of the Acoustical Society of America*, 108(6), Pages 2865-2872, 2000.
- [13] C.M.A. Vasques, R.A.S. Moreira, J. Dias Rodrigues, “Viscoelastic Damping Technologies Part I: Modeling and Finite Element Implementation”, *Journal of Advanced Research in Mechanical Engineering* 1(2), Pages 76-95, 2010.
- [14] A. Akrouf, L. Hammami, M. Ben Tahar, M. Haddar, “Vibro-acoustic behaviour of laminated double glazing enclosing a viscothermal fluid cavity”, *Applied Acoustics* 70(1), Pages 82-96, 2009.
- [15] N.W. Hagood, A.V. Flotow, “Damping of structural vibrations with piezoelectric materials and passive electrical networks”, *Journal of Sound and Vibration* 146(2), Pages 243–268, 1991.
- [16] F. dell’Isola, C. Maurini, M.A. Porfiri, “Passive damping of beam vibrations through distributed electric networks and piezoelectric transducers: prototype design and experimental validation”, *Smart Materials and Structure* 13(2), Pages 299-308, 2004.
- [17] M. Collet, K.A. Cunefare, M.N. Ichchou, “Wave motion optimization in periodically distributed shunted piezocomposite beam structures”, *Journal of Intelligent Material Systems and Structures* 20(7), Pages 787–808, 2009.

- [18] F. Casadei, M. Ruzzene, L. Dozio, K.A. Cunefare, “Broad band vibration control through periodic arrays of resonant shunts: experimental investigation on plates”, *Smart Materials and Structures* 19(1), 015002, 2010.
- [19] A. Belloli, D. Nedereberger, S. Pietrzko, M. Morari, P. Ermanni, “Structural vibration control via rl-shunted active fiber composites”, *Journal of Intelligent Material Systems and Structures* 18(3), Pages 275–287, 2007.
- [20] D. Niederberger, A. Fleming, S.O.R. Moheimani, M. Morari, “Adaptive multi-mode resonant piezoelectric shunt damping”, *Smart Materials and Structures* 13(5), Pages 1025–1035, 2004.
- [21] D. Guyomar, A. Faiz, L. Petit, C. Richard, “Wave reflection and transmission reduction using piezoelectric semipassive nonlinear technique”, *The Journal of the Acoustical Society of America* 119(1), Pages 285–298, 2006.
- [22] J. Ducarne, O. Thomas, J.-F. Deü, “Structural vibration reduction by switch shunting of piezoelectric elements: modeling and optimization”, *Journal of Intelligent Materials Systems and Structures* 21(8), Pages 797–816, 2010.
- [23] W. Larbi, J.-F. Deü, M. Ciminello, R. Ohayon, “Structural-acoustic vibration reduction using switched shunt piezoelectric patches: a finite element analysis”, *Journal of Vibration and Acoustics* 132(5), 051006, 2010.
- [24] O. Thomas, J.-F. Deü, J. Ducarne, “Vibrations of an elastic structure with shunted piezoelectric patches: efficient finite elements formulation and electromechanical couplings coefficients”, *International Journal for Numerical Methods in Engineering* 80(2), Pages 235–268, 2009.
- [25] J.-F. Deü, W. Larbi, R. Ohayon, “Piezoelectric structural acoustic problems: Symmetric variational formulations and finite element results”, *Computer Methods in Applied Mechanics and Engineering*, 197(19-20), Pages 1715-1724, 2008.

- [26] W. Larbi, J.-F. Deü, R. Ohayon, R. Sampaio “Coupled FEM/BEM for control of noise radiation and sound transmission using piezoelectric shunt damping”, *Applied Acoustics*, 86, Pages 146-153, 2014.
- [27] Z. Fan, “Transient vibration and sound radiation of a rectangular plate with viscoelastic boundary supports”, *International Journal for Numerical Methods in Engineering*, 51, Pages 619-630, 2001.
- [28] K. Bouayeda, M.A. Hamdi, “Finite element analysis of the dynamic behavior of a laminated windscreen with frequency dependent viscoelastic core”, *Journal of the Acoustical Society of America*, 132(2), Pages 757-766, 2012.
- [29] H.J.-P. Morand and R. Ohayon, “Fluid-Structure Interaction”, Wiley, New York, 1995
- [30] R. Ohayon, “Reduced models for fluid-structure interaction problems”, *International Journal for Numerical Methods in Engineering*, 60(1), Pages 139-152, 2004.
- [31] R. Panneton, N. Atalla, “Numerical prediction of sound transmission through finite multilayer systems with poroelastic materials”, *Journal of the Acoustical Society of America*, 100(1), Pages 346-354, 1996.
- [32] W. Larbi, J.-F. Deü, R. Ohayon, “Finite element formulation of smart piezoelectric composite plates coupled with acoustic fluid”, *Composite Structures*, 94(2), Pages 501-509, 2012.
- [33] T. G. H. Basten , P. J.M. Van Der Hoogt, R. M. E. J. Spiering, H. Tijdeman “On the acousto-elastic behaviour of double-wall panels with a viscothermal air layer”, *Journal of Sound and Vibration*, 243(4), 699-719, 2001.
- [34] S. Havriliak, S. Negami, “A complex plane analysis of ϵ -dispersions in some polymer systems”, *Journal of Polymer Science Part C: Polymer Symposia*, 14(1), Pages 99-117, 1966.
- [35] Y. Koutsawa, W.L. Azoti, S. Belouettar, R. Martin, E. Barkanov “Loss behavior of viscoelastic sandwich structures: A statistical-continuum multi-scale approach”, *Composite Structures*, 94(4), Pages 1391-1397, 2012.